

# DPW-8/AePW-4 Buffet Working Group: An Overview of Mini Workshops 1 and 2

Sansica Andrea\*

*Japan Aerospace Exploration Agency, JAXA Chofu Aerospace Center, Chofu, Japan*

Brent W Pomeroy<sup>†</sup> and Bret Stanford<sup>‡</sup>

*National Aeronautics and Space Administration (NASA), NASA Langley Research Center, Hampton, VA, United States*

Daniella Raveh<sup>§</sup> and Hadar Ben-Gida<sup>¶</sup>

*Technion - Israel Institute of Technology, Haifa, Israel*

This manuscript presents the findings from the joint DPW-8/AePW-4 Buffet Working Group regarding Test Case 1, focused on buffet conditions for the ONERA OAT15A supercritical airfoil. A total of ten angles of attack at both pre- and post-buffet onset conditions have been selected for freestream Mach and Reynolds numbers of  $M = 0.85$  and  $Re = 3 \times 10^6$ , respectively. The study is divided into steady and unsteady analyses. For steady simulations, significant scatter was observed in the results, highlighting the lack of grid convergence across different turbulence models and grid types. Different turbulence models showed significant deviations in aerodynamic coefficients, with a shock-wave predicted farther downstream than the experimental observations. Although unsteady simulations, including URANS and Hybrid RANS/LES models, provided improvements in predicting shock location and behavior, they still exhibited discrepancies in fluctuation amplitudes and locations. Test Case 1 has provided valuable lessons in numerical methods, computational resources, and collaborative efforts. As the Working Group prepares for Test Case 2 involving full-aircraft simulations, careful consideration of unsteady calculation costs, grid sensitivity studies, and time-integration setups will be crucial for achieving meaningful results.

## I. Nomenclature

$AR$	= aspect ratio, $AR = s/c$
$c$	= chord
$C_D, C_L, C_M$	= drag, lift and pitching moment coefficients
$C_p$	= pressure coefficient
$M$	= Mach number
$N$	= number of degrees of freedom
$Re$	= Reynolds number
$P_{st}, P_{tot}$	= static and total pressure
$s$	= span
$T_{st}$	= static temperature
$(x, y, z)$	= streamwise, wall-normal and spanwise coordinates
$\alpha$	= angle of attack or incidence

\*Researcher, Fundamental Technology Research Unit, Aviation Technology Directorate, 7-44-1 Jindaiji Higashi-machi, Chofu-shi, Tokyo 182-8522, Japan

<sup>†</sup>Computational Aerodynamics Research Engineer, Configuration Aerodynamics Branch, NASA Langley Research Center, Hampton, VA, United States, and AIAA Senior Member.

<sup>‡</sup>Aeroelasticity Research Engineer, Aeroelasticity Branch, NASA Langley Research Center, Hampton, VA, United States, and AIAA Senior Member.

<sup>§</sup>Professor/Dean, Faculty of Aerospace Engineering, Haifa 3200003, Israel, AIAA Senior Member.

<sup>¶</sup>Research Fellow, Faculty of Aerospace Engineering, Haifa 3200003, Israel, AIAA Senior Member.

## II. Introduction

OVER more than two decades, the American Institute of Aeronautics and Astronautics (AIAA) Drag Prediction Workshop (DPW) and Aeroelastic Prediction Workshop (AePW) have aimed at advancing computational methods in aerospace engineering. DPW focuses on improving drag prediction techniques, where participants benchmark their computational methods for estimating forces and moments on aircraft at defined conditions. The goal is to enhance drag prediction accuracy to allow engineers to optimize aircraft design for fuel efficiency, performance, and range, reducing the cost of operation and environmental impact. AePW, on the other hand, focuses on predicting aeroelastic phenomena, such as flutter, vibration, and structural deformations, which occur due to the interaction between aerodynamic forces and structural dynamics. Participants in AePW also work on validating their tools for predicting these behaviors in various geometries relevant to aviation to improve safety, performance, and reliability. Both workshops foster collaboration among researchers, industry professionals, and government agencies, facilitate knowledge exchange, identify best practices, and push the boundaries of computational prediction techniques in aerospace engineering. Summaries of the last editions of both DPW and AePW can be found in [1] and [2–5], respectively.

Given the similarities in focus and objectives, the two workshops recently decided to join forces in a collaborative multidisciplinary framework that seeks to leverage the expertise of the two communities. Some of the working groups of the 8<sup>th</sup> DPW (DPW-8, <https://aiaa-dpw.larc.nasa.gov/>) and 4<sup>th</sup> AePW (AePW-4, <https://nescacademy.nasa.gov/workshops/AePW4/public>) are in fact run jointly to boost cross-pollination between the two workshops. The workshop is divided into seven working groups, each one focusing upon a technical topic while using a variety of tools. Two of these working groups are DPW-centric, three are AePW-centric, and two are hybrid. One of these hybrid groups, the Buffet Working Group, is of interest in this manuscript (<https://aiaa-dpw.larc.nasa.gov/WorkingGroups/Group3/group3.html>). Buffet is a phenomenon that occurs on aerodynamic surfaces of a variety of aerospace vehicles - such as main wings - that fly in the transonic speed regime. Usually referred to as “turbulent transonic buffet”, it involves the onset of large, unsteady aerodynamic forces and structural vibrations, caused by the complex interaction between shock waves and turbulent boundary layers [6, 7]. Because of the unsteady characteristics of both flow and structural dynamics, buffet represents a very challenging problem for both DPW and AePW communities. The objective of this joint working group is to identify the nature of pre- and post-buffet flight regimes with unsteady computational fluid dynamics (CFD). Simulations are performed on both experimentally-measured deformations and with coupled fluid/structure interactions (FSIs).

The test cases selected for the buffet working group are the following:

- Test Case 1: ONERA OAT15A Transonic Airfoil with Steady and Unsteady CFD
- Test Case 2: Common Research Model Unsteady CFD with Committee-Supplied Deformed Wing Geometry
- Test Case 3: Common Research Model Unsteady CFD with Unsteady Fluid/Structure Interaction

The objective of this paper is to provide an overview for Test Case 1. The overview summarizes the data submissions gathered for the two mini-workshops held at AIAA Scitech in January 2025 and online in May 2025.

The manuscript is structured as follows: reference geometry and experimental data are given in Section III; the requirements for Test Case 1 are described in Section IV; the committee-provided grids are detailed in Section V; participants who submitted data are reported in Section VI; the results are summarized in Section VII and some conclusions and perspective future work are delineated in Section VIII.

## III. Geometry and Experimental Data Description

The reference data used for Test Case 1 correspond to the experiments carried out in the continuous closed-circuit transonic S3Ch Wind Tunnel of the ONERA-Meudon Center by Jacquin et al. [8]. The geometry corresponds to the ONERA OAT15A supercritical airfoil, represented in Figure 1 and openly available, with conditions, at <https://aiaa-dpw.larc.nasa.gov/geometry.html#oat>.

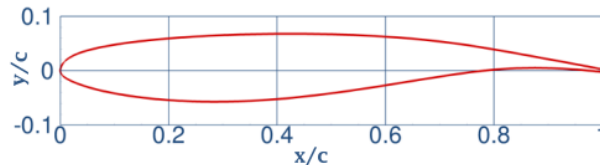


Fig. 1 Normalized ONERA OAT15A airfoil.

The airfoil has a chord length of  $c = 230\text{ mm}$ , with a relative thickness of 13% and blunt trailing-edge with a thickness of 0.5% the chord length. The profile is extruded in the spanwise direction and flash-mounted on the wind-tunnel side-walls. With a span width of  $s = 780\text{ mm}$ , the model aspect ratio is  $AR = s/c \approx 3.4$ . A tripping strip was located at 7% of the chord downstream of the leading-edge on both pressure and suction sides to trigger transition. For the selected pressure and temperature at stagnation conditions of  $P_{st} = 10^5\text{ Pa}$  and  $T_{st} = 300\text{ K}$ , the corresponding Reynolds number based on the airfoil chord is  $Re = 3 \times 10^6$ . For a Mach number of  $M = 0.73$ , the angle of attack ( $\alpha$ ) was varied between 1.36 and 3.9 degrees. The model is equipped with 68 static pressure taps and 36 unsteady Kulite pressure transducers that have been used to extract the mean and root-mean-square (rms) reference data, as well as power spectral densities (PSDs). For some selected cases, oil-flow and Schlieren visualizations were also provided. No forces and moments were provided. A subset of reference experimental data is available on <https://aiaa-dpw.larc.nasa.gov/experiment.html>. While there has been experimental evidence of three-dimensional (3D) effects in the corner regions, the experimental data are assumed to be span-independent. Based on the analysis of the unsteady experimental measurements, buffet onset was determined at the angle of attack  $\alpha = 3.10^\circ$ .

#### IV. Test Case Description

Test Case 1 is based on the ONERA OAT15A experiments described above and aims at functioning as a workshop-wide validation test for CFD analysis. Within the context of the Buffet Working Group, Test Case 1 is however further divided into two sub-cases (for steady and unsteady CFD, respectively) and supplementary requirements are added relative to the rest of the workshop. The main information and requirements for Test Case 1 are reported in Table 1. A detailed description is given in <https://aiaa-dpw.larc.nasa.gov/WorkingGroups/Group3/TestCases/buffet-case1-v3.pdf>.

The participants were encouraged to employ their own best practices, but some guidelines were provided in terms of grids and simulation settings. Simulations settings were generally left up to the user and multiple datasets could be submitted, but turbulence model versions based on Spalart-Allmaras (SA) formulation [9] were recommended.

The main goal of Test Case 1 was to establish the accuracy of each solver before moving on to the CRM full-aircraft simulations.

**Table 1 Overview of Test Case 1: Buffet Working Group supplemental requirements in bold.**

Case	Method	$M$	$Re$	$T_{st}$ (K)	$P_{tot}$ (kPa)	$\alpha$ ( $^\circ$ )
1a	Steady	0.73	$3 \times 10^6$	271	102.4	1.36, 1.50, 2.50, 3.00, 3.10, <b>3.25, 3.40, 3.50, 3.60, 3.90</b>
<b>1b</b>	<b>Unsteady</b>	<b>0.73</b>	<b><math>3 \times 10^6</math></b>	<b>271</b>	<b>102.4</b>	<b>1.36, 1.50, 2.50, 3.00, 3.10, 3.25, 3.40, 3.50, 3.60, 3.90</b>

#### V. Computational Grids

Results were submitted using a combination of committee-supplied grids and user-generated grids. Both Cadence and Helden Aerospace provided committee-supplied grids, which users were strongly encouraged to utilize. Previous DPW, in particular DPW-IV and DPW-V, highlighted the need for high-quality comparisons on consistent grids. These common grids were released on the DPW website for participant use. Gridding guidelines were developed to ensure workshop-wide consistency when comparing grid resolutions. While participants were encouraged to utilize the committee-supplied grids, custom grids were permissible. For Reynolds-Averaged Navier-Stokes (RANS) approaches, one-cell wide six-member grid topologies were provided to perform purely two-dimensional (2D) simulations. Higher fidelity methods, like hybrid RANS/Large Eddy Simulations (LES) or wall-modeled LES (WMLES), were recommended to use 3D span-periodic airfoils with 10% chord span-width, although grids were not supplied. Best practices for RANS analysis has been well documented in the literature, but some disagreement exists regarding grid requirements for scale-resolving schemes. Consequently, the committee encouraged users to develop grids for these unsteady solvers to help develop recommended best practices. Unfortunately, many participants did not use the committee-supplied grids and instead submitted data with user-generated grids, and only one participant (ONERA) submitted custom grids for public use. As key grid metric quantities were not shared, it is extremely difficult to compare submissions that used the committee-supplied grids and those that generated custom grids. As many submissions used these committee-supplied grids, a description of the common grids is warranted in this paper.

## VI. Participants List

Participation in DPW-8 is open to any individual, group, or organization willing to carry out the calculations in accordance with the specifications provided by the organizing committee. For case 1, a total of 74 datasets were submitted by 18 participants. Broken down by method and grid, these submissions are:

Method	Grid
RANS: 56 datasets URANS: 11 datasets Hybrid RANS/LES: 5 datasets WMLES: 1 dataset Adaptive Euler: 1 dataset	Cadence structured: 15 datasets Cadence unstructured: 35 datasets Custom: 21 datasets Helden Aerospace: 3 datasets

The full list of participants in given in Table 2. The turbulence model nomenclature proposed in NASA Turbulence Modeling Resource website (<https://turbmodels.larc.nasa.gov/>) is used. All participants were asked to submit forces & moments and pressure coefficient distributions. Convergence histories for Test Case 1a and time-averaged and rms components, unsteady pressure probe histories and corresponding PSD at  $x/c = 45$  (Kulite 7) for Test Case 1b were also requested.

**Table 2 List of participants to case 1 from Scatter and Buffet working groups.**

ID	Team	Organization	Solver	Method	Turbulence Model	Grid
002	Mestriner	Embraer	CFD++	RANS	SA, SA-RC-QCR SST	Cadence structured, Cadence unstructured, HeldenAero
004	Pomeroy, Jamal, Pandya	NASA (Langley CAB)	USM3D-ME	RANS	SA, SA-R, SA-QCR2000	Cadence unstructured
005	Housman	NASA (Ames)	LAVA	RANS URANS HRLES	SA-neg, SA-neg-RC-comp	Cadence structured Deck extruded
006	Jirasek	US Air Force Academy	Loci/CHEM	RANS, URANS, HRLES	k-w-Wilcox 1998k, SST	Cadence unstructured
007	Sansica, Lusher, Matsuzaki	JAXA	FaSTAR	RANS, URANS	SA-noft2, SA-noft2-R, SA-noft2-R-QCR, SST	Cadence structured, Custom
008	Batten, Bachchan, Kovvali	Metacomp	CFD++	RANS, URANS, HRLES	SA-neg-RC-QCR	Cadence structured, Deck extruded
009	Petropoulos, Sartor	ONERA (DAAA)	elsA	RANS	SA, SST	Cadence structured, Cadence unstructured, Custom, HeldenAero
010	Goc, Clark	Boeing (BCA Technology)	charLES	WMLES	Dynamic Smagorinski	Custom
012	Chwalowski Massey Jacobson	NASA (Langley AEL)	FUN3D	RANS, URANS	SA-neg, SA-neg-comp SA-neg-comp-QCR, SA-neg-RC-comp-QCR, SST-comp-QCR	Cadence unstructured, Custom adapted
014	Udupa, Venkatraman	IIS	SU2	RANS, URANS	SA-Edwards	Cadence unstructured
018	Darbyshire, Wainwright, Allan	Zenotech	zCFD	RANS	SA-neg, SST-V-2003	Cadence unstructured
021	Lamberson, Lynch, Jamal, Pomeroy	CREATE-AV NASA Langley	Kestrel	RANS, URANS	SA-RC-QCR	Cadence unstructured
023	Arnould, Radigue, Laurendau	Polytechnique Montreal	CHAMPS	RANS	SA	Cadence unstructured
024	Nash, Timme	Univ. of Liverpool	TAU	RANS	SA-neg	Cadence unstructured
026	Eldridge-Allegra, McGowan	Corvid Tech.	Raven	RANS	SA, SA-comp	Cadence unstructured
027	Candon, Gerner	RMIT	N/A	RANS, URANS	SA, SA-C, SST, SST-C	Cadence structured
032	Jansson	KTH	N/A	Adaptive Euler	N/A	Custom

## VII. Results

Data submissions were collected on the shared Github repository available at <https://github.com/Drag-Prediction-Workshop/DPW8-Buffet>. While some updates were requested, the results shown here correspond to those submitted before 2025 May 16th. Steady (Test Case 1a) and unsteady (Test Case 1b) submissions are reported separately in the following subsections. Some comparisons between steady and unsteady results are also given for those participants who submitted both steady and unsteady data. In the attempt to find possible trends among the submissions, the same plots are repeated by grouping and color-coding the solutions based on method, turbulence model or grid type. Experimental reference data are also added, whenever available. Those datasets that presented formatting issues have been excluded from the analysis.

### A. Test Case 1a: Steady (RANS) Results

#### 1. Grid Study

Based on the experimentally determined buffet onset, the angles of attack  $\alpha = 1.50, 3.10$  and  $3.90^\circ$  have been selected as representative cases for pre-onset, onset and post-onset conditions for the analysis of the grid sensitivity. Aerodynamic coefficients for different grid resolutions (with  $N$  number of degrees of freedom) are given for the aforementioned angles of attack in Figures 2, 3 and 4, respectively. The same parameters are presented in two plots, based on either turbulence model (left column) or grid type (right column). The first thing to notice is that a unique grid converged solution cannot be found by neither turbulence model nor grid type grouping for any of the angles of attack reported. For all angles of attack, there is a slight tendency of SA-based results to give higher values of  $C_D$  and  $C_L$ , and decreased magnitude of  $C_M$  compared to those given by models including QCR corrections. Few contributions with  $k - \omega$  or SST models prevent from drawing any qualitative conclusion. No general trends can be discerned by looking at the results grouped by grid type. By considering solutions for the finest grid level available, very large differences can be seen among the submissions. This scatter increases for higher angles of attack and is estimated to be about 10, 50 and 90  $C_D$  counts and 35, 95 and 120  $C_L$  counts for  $\alpha = 1.50, 3.10$  and  $3.90^\circ$ , respectively. While the scope of this working group was not to reduce scatter, it should be highlighted that most of the contributions do not show grid converged results.

#### 2. Polars

Forces and moments polars for Test Case 1a are shown in Figure 5. Similarly to what was done in the previous section, the same parameters are reported in two plots, based on either turbulence model (left column) or grid type (right column). Once again, it is difficult to identify a clear trend based on turbulence model or grid type and large scatter exists. However, similarly to what was seen in the grid study plots, SA-based results tend to provide higher values of  $C_D$  and  $C_L$ , and decreased  $C_M$  compared to those given by models including QCR corrections. For the lowest angle of attack, about 30  $C_D$ -counts and 40  $C_L$  counts of difference exist among participants. This discrepancy increases to 75  $C_D$ -counts and 140  $C_L$  counts for the highest angle of attack. It should be noted that these scatter estimates are slightly higher than those shown in the previous section because the polars correspond to grid level 4 resolutions. As mentioned previously, the objective of this working group was not to reduce scatter, as this was the goal of the separate Source of Scatter Working Group. While it is expected for RANS models to under-perform in the presence of largely separated flows, a certain level of alert should be however raised, as these values of scatter are similar to those found for the full-aircraft RANS calculations in DPW-7 [1].

#### 3. Pressure Coefficient Distributions

Sectional pressure coefficient distributions colored by turbulence model are plotted against the experimental measurements for  $\alpha = 2.50, 3.00, 3.10, 3.25, 3.50$  and  $3.90^\circ$  in Figure 6. For pre-buffet conditions ( $\alpha < 3.10^\circ$ ), SA-based models including rotation, curvature and QCR correction have a general tendency to predict the shock much further downstream as compared to the experiments. Things improve for SA-based models that include the compressibility correction, but differences still exist. At post-buffet conditions, the RANS solutions still predict a very sharp pressure gradient due to the (steady) shock-wave. The experiments, however, show a pressure gradient that is “smeared” over a large streamwise range, due to the oscillating behavior of the shock. The discrepancies of some of the RANS solutions with the experiments at pre-buffet conditions do not necessarily have to be seen as a failure, since these simulations are purely 2D (i.e. one-cell wide) and do not account for any 3D effects that may be present in the

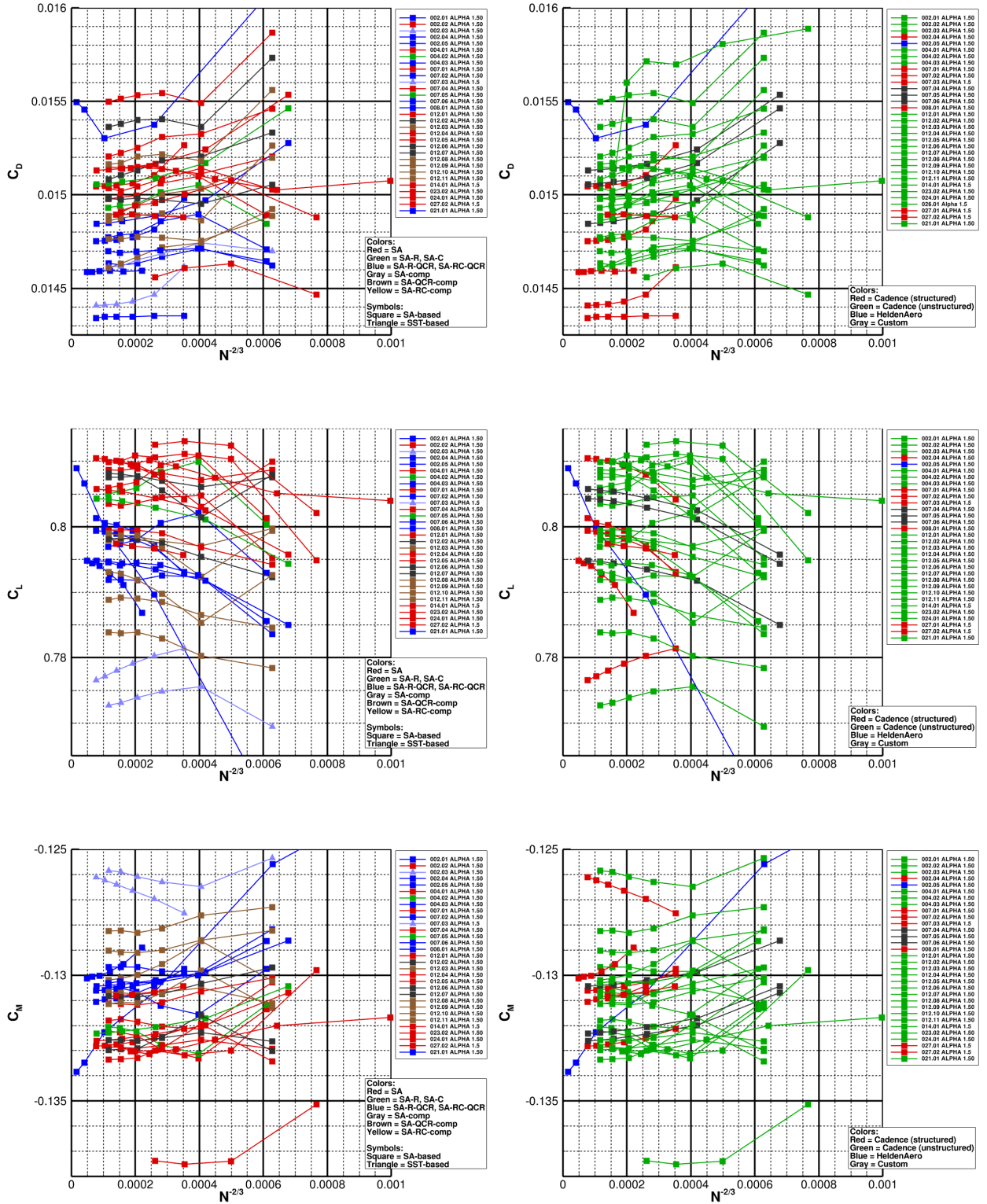


**Fig. 2 Case 1a, RANS grid study at  $\alpha = 1.50^\circ$ . The solutions are colored based on (left) turbulence model and (right) grid type.**

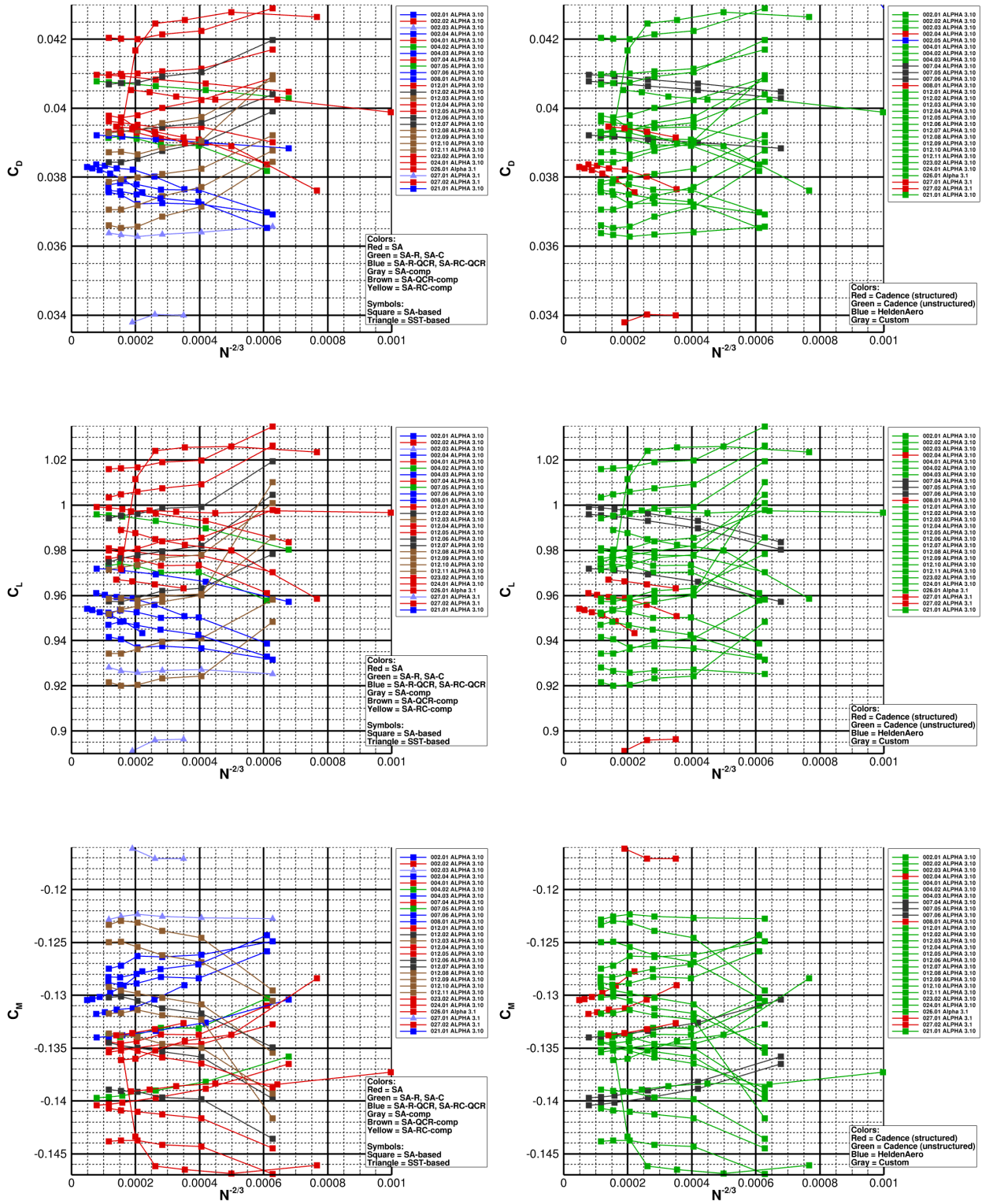
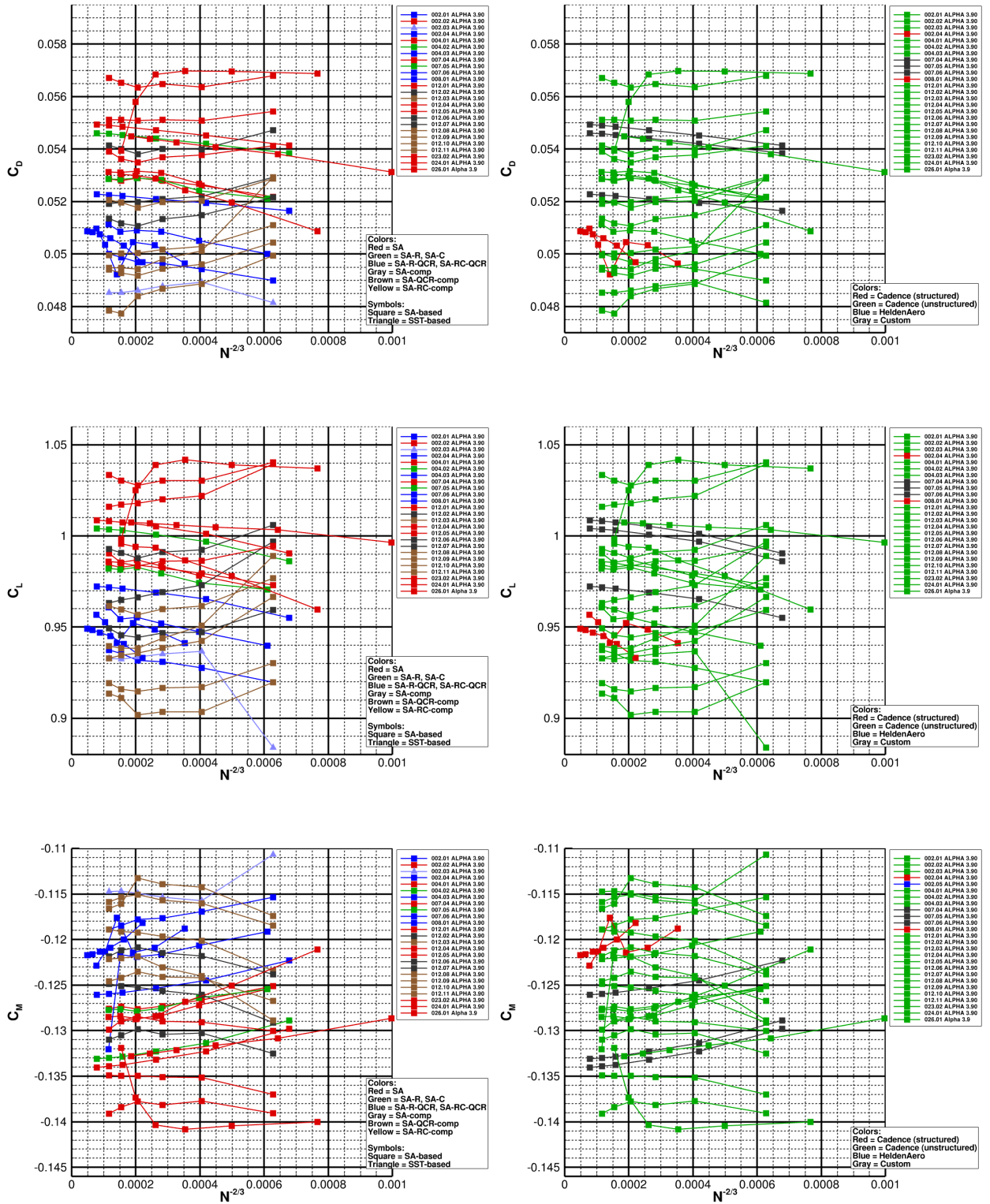


Fig. 3 Case 1a, RANS grid study at  $\alpha = 3.10^\circ$ . The solutions are colored based on (left) turbulence model and (right) grid type.



**Fig. 4 Case 1a, RANS grid study at  $\alpha = 3.90^\circ$ . The solutions are colored based on (left) turbulence model and (right) grid type.**

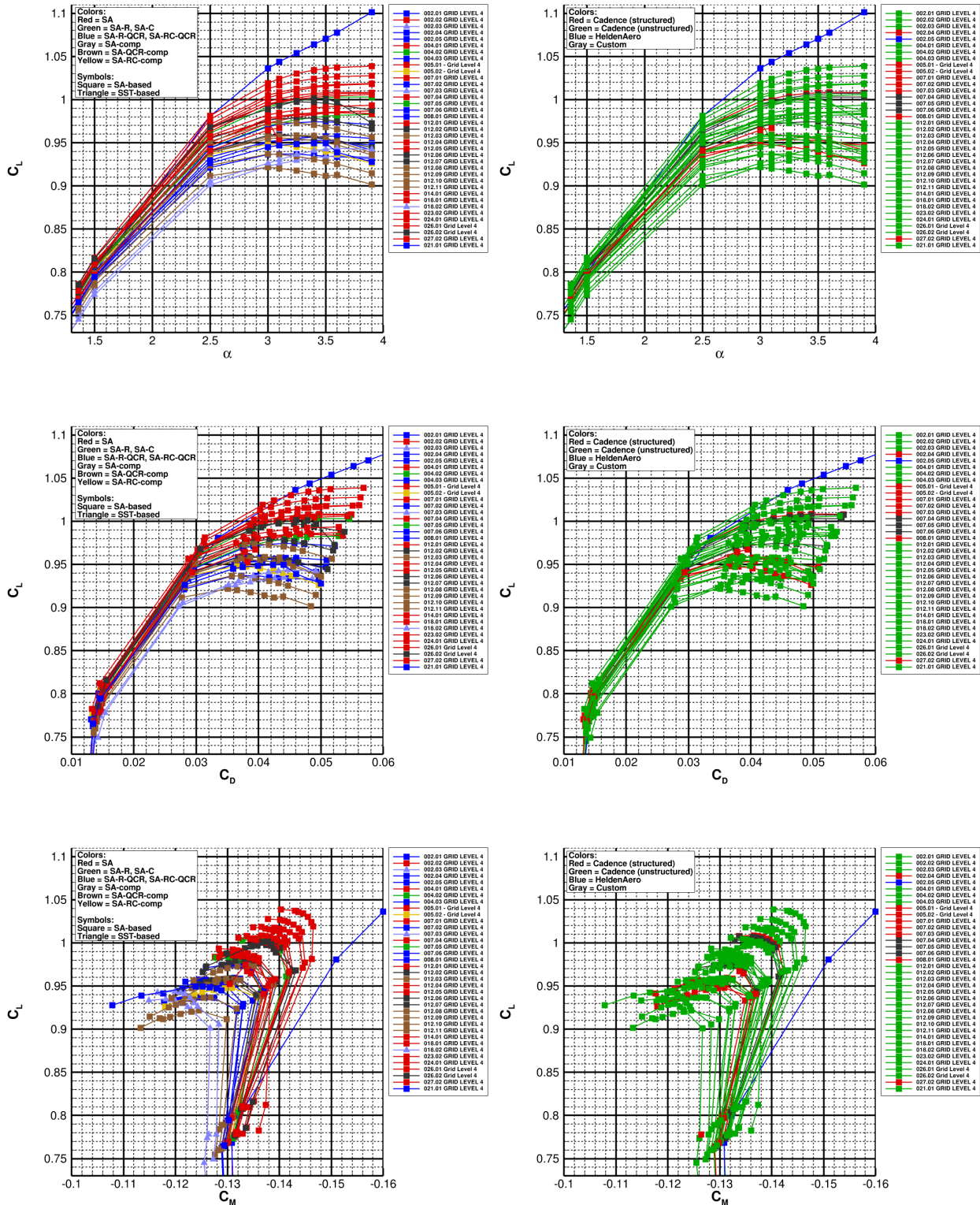
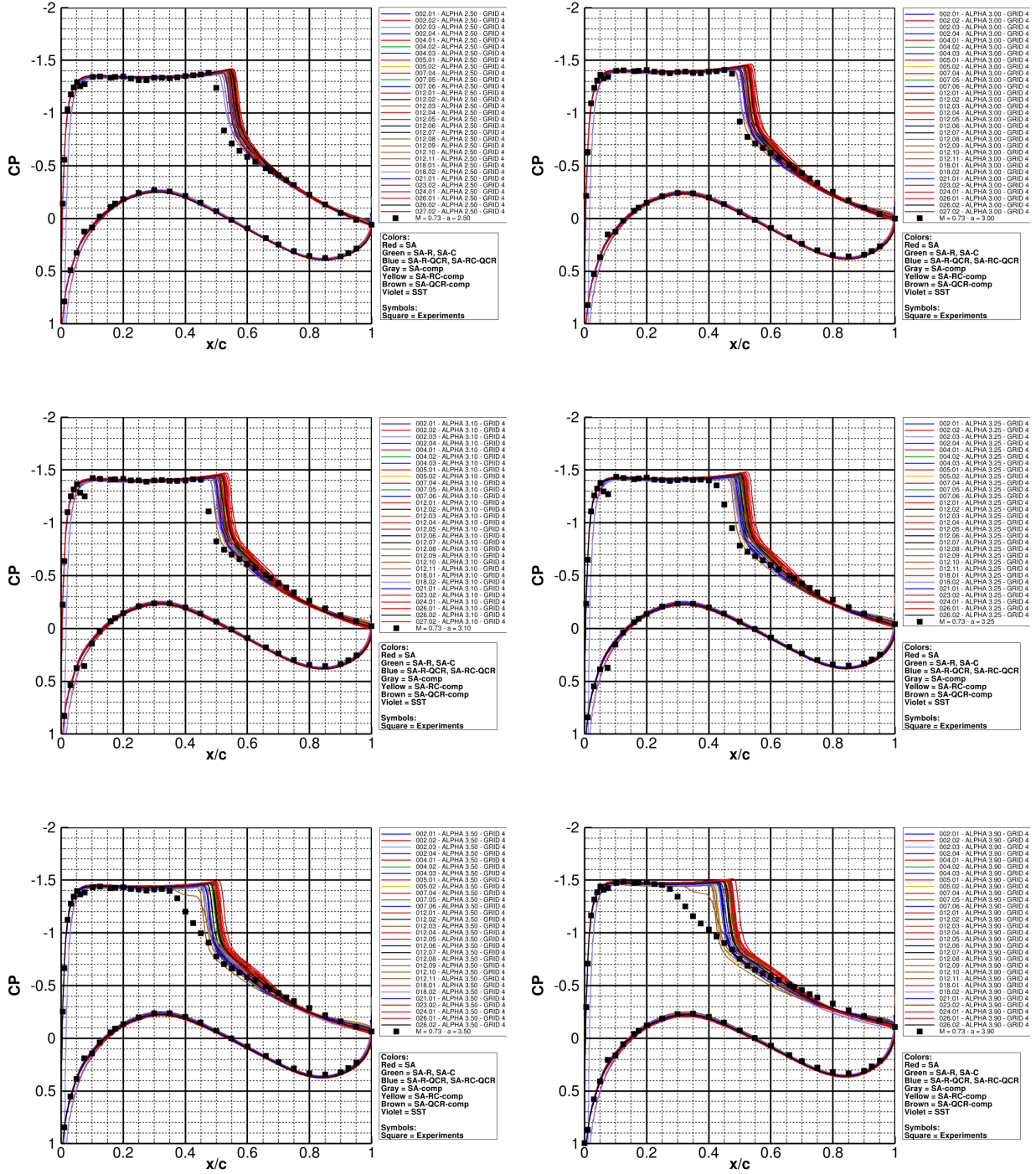


Fig. 5 Case 1a, RANS forces and moments polar plots. The solutions are colored based on (left) turbulence model and (right) grid type.

experiments.



**Fig. 6 Case 1a, RANS  $C_P$  distributions for  $\alpha = 2.50^\circ$  (top left),  $3.00^\circ$  (top right),  $3.10^\circ$  (middle left),  $3.25^\circ$  (middle right),  $3.50^\circ$  (bottom left) and  $3.90^\circ$  (bottom right) . The solutions are colored based on turbulence model.**

## B. Test Case 1b: Unsteady Results

### 1. Polars

Despite being the main objective of the working group, only about 20% of the submissions correspond to unsteady calculations. Large majority of the unsteady data sets consist of URANS calculations, but results from higher-fidelity methods like Hybrid RANS/LES and WMLES were also submitted. Left plots in Figure 7 show the polars for all Test Case 1b submissions colored by numerical method. The reader should be reminded that these forces and moments are time-averaged. Similar conclusions on general trends and large scatter observed for the RANS results can be repeated for the unsteady results. The higher fidelity methods (Hybrid RANS/LES and WMLES) do however indicate a  $C_{L,max}$  peak at around  $\alpha = 3.1^\circ$ , the angle of attack for which the experiments indicated buffet onset. For some selected participants who provided both steady and unsteady calculations, the polars for both RANS (square symbols) and unsteady (triangle symbols) results are colored by participant ID and reported on the right plots in Figure 7. Considering buffet onset at  $\alpha = 3.1^\circ$ , one would expect - at least for the RANS vs URANS contributions - that steady and unsteady results would be the same for the low angles of attack. Differences however exist and may be due to either insufficient iterative convergence of the RANS solutions or excessively short statistics collection times for the unsteady calculations. While this needs further investigations, the lack of specific guidelines on how to determine initial transients, appropriate statistics collection times and initial solution to start the unsteady calculations from does not guarantee consistency among participants. In the light of this, criteria may be added for future test cases. Another aspect to emphasize is the values of the aerodynamic forces of the unsteady calculations with respect to their steady counterparts. Generally speaking, due to the oscillations of the shock-wave and related change in separation size, for the same angle of attack the time-averaged unsteady forces should be lower with respect to the (steady) RANS ones. This is however not true for all reported solutions, calling for more in-depth analysis.

### 2. Pressure Coefficient Distributions

Time-averaged  $C_P$  distributions colored by numerical method are shown in Figure 8 for  $\alpha = 2.50, 3.00, 3.10, 3.25, 3.50$  and  $3.90^\circ$  along with the experimental results. Given the scarce number of contributions, it is difficult to make definite conclusions. The time-averaged CFD solutions move closer to the experimental shock location but are still found to be too far downstream. Notable exception is the SST-comp-QCR2020 contribution that falls right on top of the reference data. At post-buffet onset conditions, the smeared shock distributions are qualitatively well reproduced. No striking differences can be seen in the higher fidelity methods, except for an over-prediction of the suction downstream of the shock for the Hybrid RANS/LES methods. For the same angles of attack, the experimental  $C_P$ -rms distributions are plotted against the numerical ones in Figure 9. Hybrid RANS/LES and SA-based (suspicion here is that some "-comp" corrections were not reported by the participants) URANS contributions show large pressure fluctuations at low angles of attack, indicating that buffet onset is predicted too early. URANS calculations with SA-QCR and SST report instead weak fluctuations and delayed onset. URANS results present difficulties in predicting the correct streamwise shock excursion and the fluctuation peak location, but behave well downstream of the interaction. The Hybrid RANS/LES methods instead better capture the fluctuations near the interactions but overestimate them in the aft part of the airfoil. The WMLES results at the highest angle of attack present some differences in the upstream part of the interaction, but then generally agree well from the fluctuations peak location.

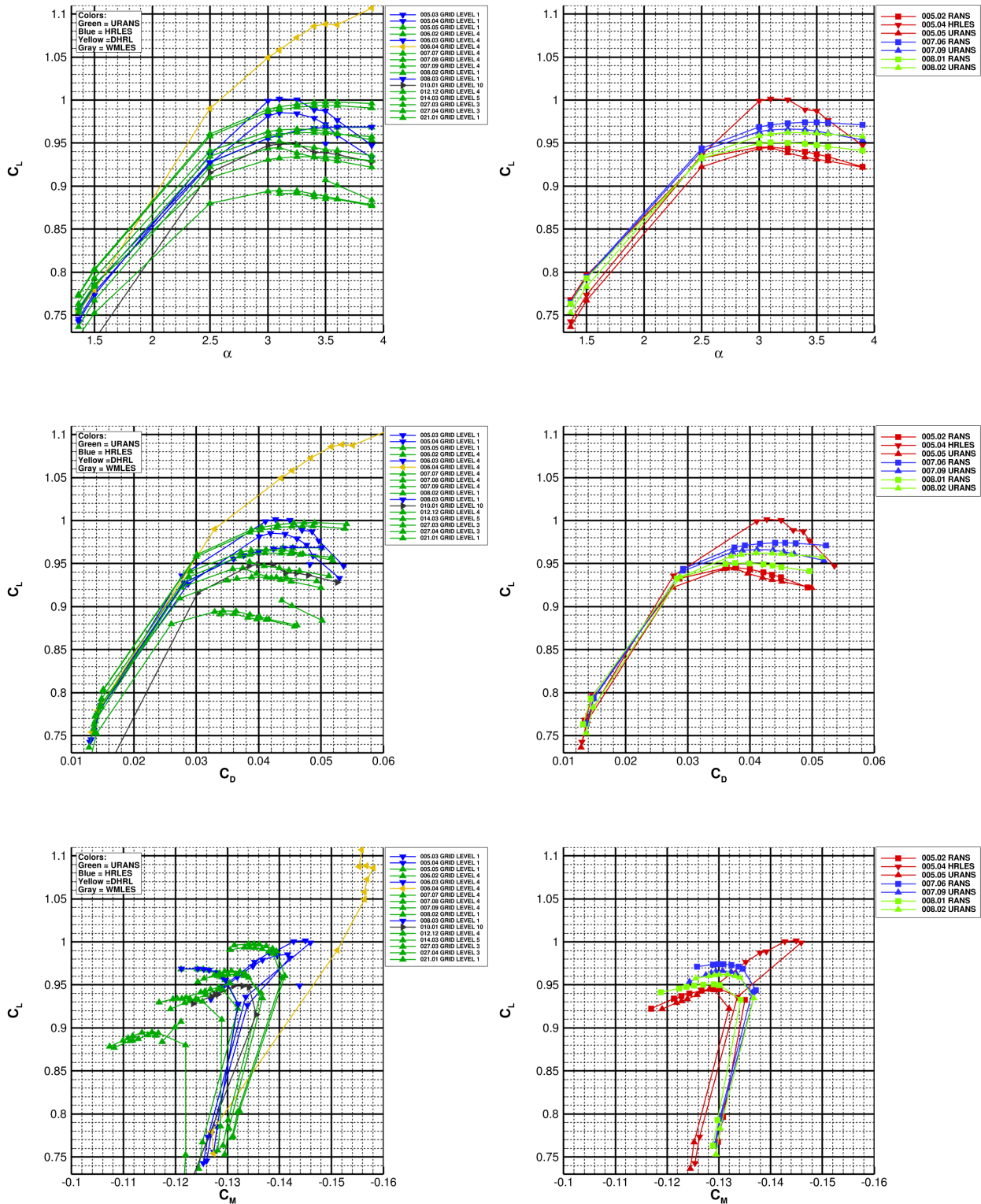
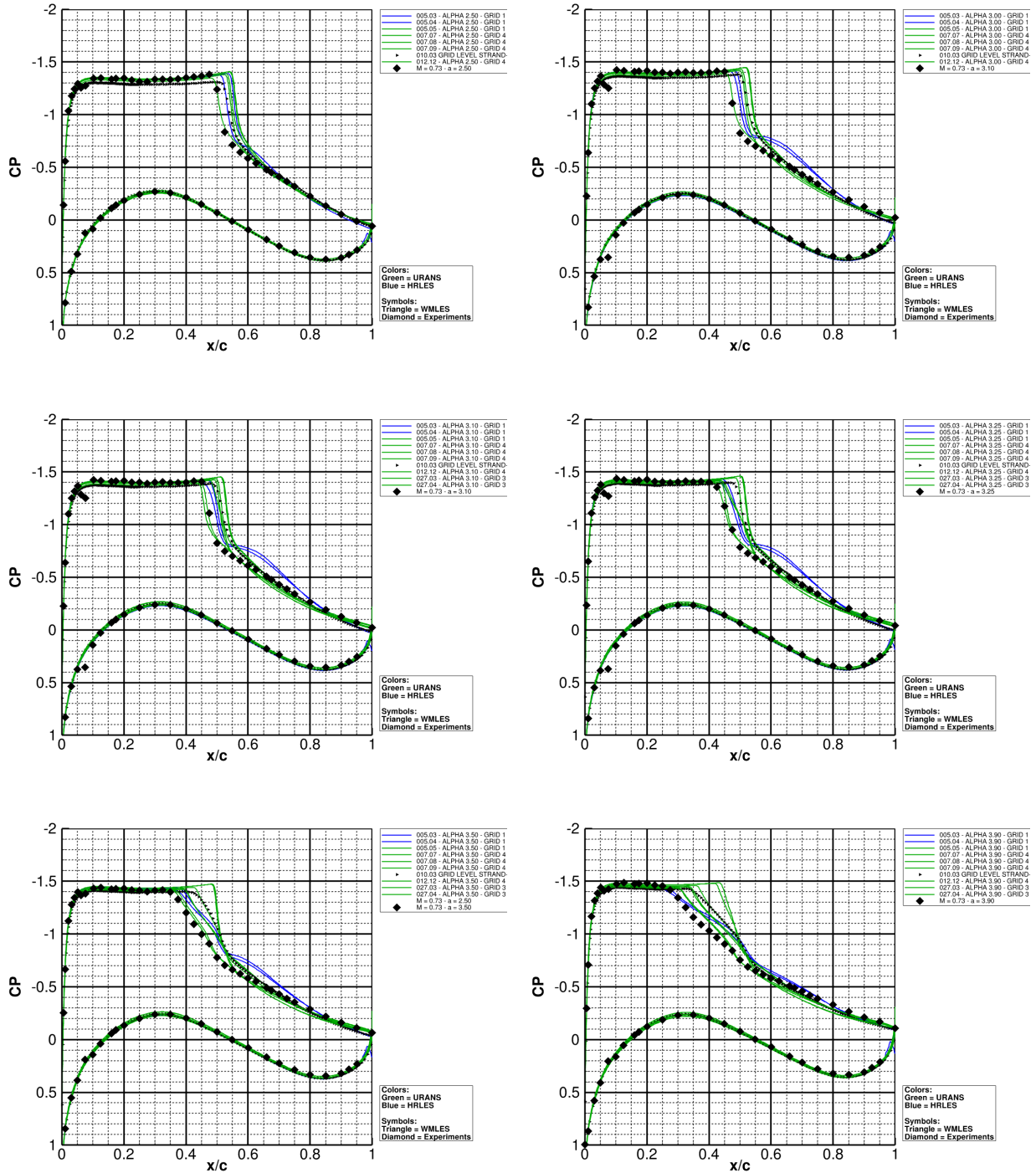
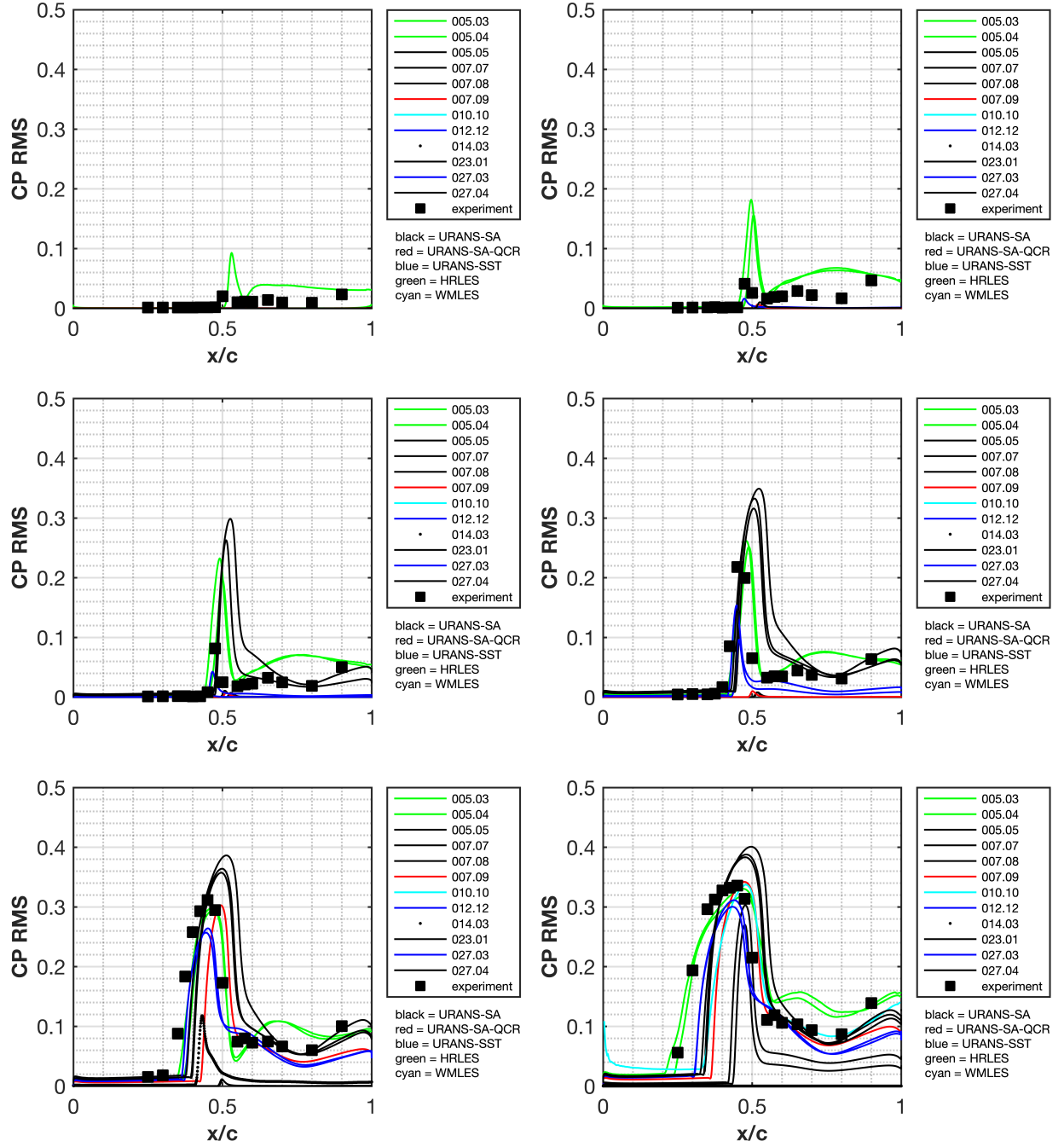


Fig. 7 Case 1b, time-averaged forces and moments polars. Left plots: solutions colored based on method; Right plots: steady (square symbols) and unsteady (triangle symbols) solutions colored based on participant ID (for those who submitted data for both cases 1a and 1b).



**Fig. 8** Case 1b, time-averaged  $C_P$  distributions for  $\alpha = 2.50^\circ$  (top left),  $3.00^\circ$  (top right),  $3.10^\circ$  (middle left),  $3.25^\circ$  (middle right),  $3.50^\circ$  (bottom left) and  $3.90^\circ$  (bottom right). The solutions are colored based on method.



**Fig. 9** Case 1b,  $CP\text{-}rms$  distributions for  $\alpha = 2.50^\circ$  (top left),  $3.00^\circ$  (top right),  $3.10^\circ$  (middle left),  $3.25^\circ$  (middle right),  $3.50^\circ$  (bottom left) and  $3.90^\circ$  (bottom right). The solutions are colored based on participant ID.

## VIII. Conclusions and Future Work

The present manuscript summarizes the efforts of the joint DPW-8/AePW-4 Buffet Working Group for Test Case 1. The geometry and experimental data refer to the experiments carried out at ONERA-Meudon Center in the transonic S3Ch wind tunnel on the ONERA OAT15A supercritical profile at buffet conditions [8]. For the Buffet Working Group, Test Case 1 is sub-divided into steady and unsteady analyses. A total of 74 datasets were provided by 18 teams. Despite the main objective of the working group, only 18 datasets concerning unsteady calculations were submitted. While a few higher fidelity submissions were provided, the large majority consisted of URANS solutions. This indicates a certain reluctance of the community to perform unsteady calculations, probably due to the increased computational cost and/or difficulties in the correct setting of simulation parameters, such as those related to time-integration. Also, a large number of participants switched to custom grids, but further discussions should be promoted to understand the reasons.

For the steady part of this study, an evident conclusion is the large scatter that exists among the different submissions. While participants were encouraged to use their own best-practices and scatter reduction was out of scope, some concern stands. A general lack of grid convergence at both pre- and post-buffet conditions was found among the submissions, regardless of turbulence model or grid type. Generally speaking, SA-based results tend to provide higher (lower) values of  $C_D$  and  $C_L$  ( $C_M$ ) compared to those given by models including QCR corrections. This is also reflected in the  $C_P$  distributions, where SA-based models predict the shock-wave farther downstream. As expected, the RANS steady solutions cannot reproduce oscillating behavior of the flow at post-buffet onset conditions and show a sharp pressure gradient at the shock. The RANS results are however inaccurate even at pre-buffet onset conditions, with a shock-wave predicted downstream of the experimental measurements.

Few unsteady contributions prevent forming definite conclusions, but large scatter is also found between URANS, Hybrid RANS/LES and WMLES contributions at both pre- and post-buffet conditions. The time-averaged  $C_P$  distributions present improvements with respect to the RANS solutions and the shock location and behavior predicted by the unsteady calculations is much closer to the experimental measurements, but visible differences still exist. Consistently with past numerical studies, the  $C_P$ -rms distributions indicate that the CFD calculations struggle to predict the correct fluctuation amplitudes and location, with some models and approaches behaving better around the shock or downstream in the separated region.

Many lessons were learned in Test Case 1, both from a numerical and organizational point of view. With the full-aircraft simulations planned for Test Case 2, it is important to recognize that the cost of the unsteady calculations might become prohibitive for many participants with limited resources. An active involvement must be secured in order to have a sufficient number of contributions for drawing quantitative conclusions. Given the complexity of the geometries, it might be difficult to have a large number of contributors using custom grids. Coordination between participants will be required to provide meaningful sensitivity studies on grid and turbulence model. An important aspect to consider carefully is the time-integration setup. It will be important to promote discussions on time-integration parameters, transients and statistic collection times. The way unsteady data will be reported also requires close scrutiny to avoid inconsistencies that will result in poor comparisons.

The kind of activities related to prediction workshops always present significant challenges. Each test case has its own unique problems and the learning curve is steep. However, much is learned on the way and the efforts of the community are incommensurable. The Buffet Working Group Organizing Team would like to express sincere gratitude to all the participants who contributed valuable data and insights during the activities related to Test Case 1. The dedication and efforts were instrumental in enriching the quality of this work.

## Acknowledgments

We would like to express our sincere gratitude to the teams who generated and provided the grid data used in this study. Their dedication and expertise in developing and sharing these resources were invaluable to the success of our research. Special thanks to Claudio Pita and Carolyn Woeber from Cadence; Rick Hooker and Andrew Wick from Helden Aerospace; and Sebastian Deck, Ilias Petropoulos, and Fulvio Sartor from ONERA for their continuous support and for making their high-quality grid datasets accessible. Without their contributions, this work would not have been possible. We also acknowledge the technical staff involved in ensuring the integrity and precision of the grid data.

## References

- [1] Tinoco, E., *Summary Data from the Seventh AIAA CFD Drag Prediction Workshop*, 2023. <https://doi.org/10.2514/6.2023-3492>.

- [2] Ouellette, J. A., Massey, S., Grauer, J. A., Chin, A. W., Timmermans, H., Aalbers, J., Mkhoyan, I., and Blom, P., *Summary of Results from the Third Aeroelastic Prediction Workshop Flight Test Working Group*, 2024. <https://doi.org/10.2514/6.2024-0415>.
- [3] Chwalowski, P., McHugh, G., Massey, S., Poplingher, L., Raveh, D. E., Jirasek, A., Giannelis, N. F., Venkatraman, K., Singh, M., Ahrabi, B., and Hong, M., *Shock-Buffet Prediction Report in Support of the High Angle Working Group at the Third Aeroelastic Prediction Workshop*, 2024. <https://doi.org/10.2514/6.2024-0417>.
- [4] Chwalowski, P., Stanford, B., Jacobson, K., Poplingher, L., Raveh, D. E., Jirasek, A., Pagliuca, G., and Marcello, R., *Flutter Prediction Report in Support of the High Angle Working Group at the Third Aeroelastic Prediction Workshop*, 2024. <https://doi.org/10.2514/6.2024-0418>.
- [5] Ritter, M., Hilger, J., Ribeiro, A., Öngüt, A. E., Righi, M., Raveh, D. E., dos Santos, L. G. P., Drachinsky, A., Riso, C., Cesnik, C. E., Stanford, B., Chwalowski, P., Kovvali, R. K., Duessler, S., Cheng, K. C., Palacios, R., dos Santos, J. P., Marques, F. D., Begnini, G. R. R., Verri, A. A., Lima, J. J., de Melo, F. B., and Bussamra, F. L., *Collaborative Pazy Wing Analyses for the Third Aeroelastic Prediction Workshop*, 2024. <https://doi.org/10.2514/6.2024-0419>.
- [6] Lee, B. H. K., “Self-sustained shock oscillations on airfoils at transonic speeds,” *Progress in Aerospace Sciences*, Vol. 37, 2001, pp. 147–196. [https://doi.org/10.1016/S0376-0421\(01\)00003-3](https://doi.org/10.1016/S0376-0421(01)00003-3).
- [7] Giannelis, N. F., Vio, G. A., and Levinski, O., “A review of recent developments in the understanding of transonic shock buffet,” *Progress in Aerospace Sciences*, Vol. 92, 2017, pp. 39–84. <https://doi.org/10.1016/j.paerosci.2017.05.004>.
- [8] Jacquin, L., Molton, P., Deck, S., Maury, B., and Soulevant, D., “Experimental Study of Shock Oscillation over a Transonic Supercritical Profile,” *AIAA Journal*, Vol. 47, No. 9, 2009, pp. 1985–1994. <https://doi.org/10.2514/1.30190>.
- [9] Spalart, P., and Allmaras, S., “A one-equation turbulence model for aerodynamic flows,” *30th aerospace sciences meeting and exhibit*, 1992, p. 439. <https://doi.org/10.2514/6.1992-439>.